NATIONAL ADVISORY COMMITTEE FOR AERONAUTICS

WARTIME REPORT

ORIGINALLY ISSUED
September 1944 as
Advance Confidential Report L4I23

SIMPLE CURVES FOR DETERMINING THE EFFECTS OF COMPRESSIBILITY ON PRESSURE DROP THROUGH RADIATORS

By John V. Becker and Donald D. Baals

Langley Memorial Aeronautical Laboratory
Langley Field, Va.

NACA

WASHINGTON

NACA ACR No. L4I23 [redacted]

NATIONAL ADVISORY COMMITTEE FOR AERONAUTICS

ADVANCE CONFIDENTIAL REPORT

SIMPLE CURVES FOR DETERMINING THE EFFECTS OF COMPRESSIBILITY ON PRESSURE DROP THROUGH RADIATORS

By John V. Becker and Donald D. Baals

SUMMARY

Simple curves are presented by which the basic pressure-drop characteristics of unheated tubular radiators can be corrected to operating conditions in which the radiator is heated and in which the Mach number of the tube flow is of appreciable magnitude. The only data required for the use of the curves are the radiator dimensions, the rate of heat input, the pressure and temperature ahead of the radiator, and the rate of mass flow of air through the radiator.

The accuracy of the curves for predicting the compressibility effects for unheated radiators is confirmed by comparison with test data obtained from two independent sources. An example of the use of the curves for a typical oil-cooler installation is given.

INTRODUCTION

The pressure-drop coefficient for a cold tubular radiator, as usually determined from tests with low airspeed in the tubes, is known to be subject to correction if the radiator is operated under conditions in which an appreciable density decrease occurs as the air passes along the tube. This decrease in density may be caused by the increase in absolute temperature due to the addition of heat, by the reduction in absolute static pressure due to the pressure drop within the tube, or by both. The density decrease due to the addition of heat is important under all operating conditions, but the density decrease due to the static-pressure reduction becomes important only when the pressure drop is appreciable in comparison with the absolute static pressure - that is, when the Mach number of the tube flow becomes

[redacted]

of appreciable magnitude (reference 1). In high-speed airplanes, neglect of the Mach number effect will result in sizable underestimation of the pressure drop required to induce the necessary cooling-air flow.

A number of investigators have demonstrated that compressibility has no appreciable effect on the heat-transfer coefficient. The temperature difference on which the heat-transfer calculations at high Mach numbers must be based, however, is the difference between the wall temperature and the stagnation temperature of the cooling air rather than the true temperature of the cooling air. (See reference 2.) Test data on the heat-transfer characteristics obtained at any test Mach number may thus be used to determine the mass flow required for cooling for the design condition. In the present report the mass flow is assumed to have been so determined and the report is concerned only with the determination of the pressure drop necessary to induce the required mass flow.

The purpose of the present paper is to present curves from which the basic pressure-drop characteristics of cold radiators can be corrected to operating conditions in which the radiator is heated and the Mach number of the tube flow is of appreciable magnitude. The only requirement for the use of the curves is knowledge of the radiator dimensions, the rate at which heat is to be dissipated, the pressure and temperature ahead of the radiator, and the rate of mass flow of air through the radiator. The curves are constructed for a Mach number range from zero to the maximum attainable Mach number corresponding to existence of sonic velocity at the exits of the tubes.

A knowledge of the theory by which the curves are derived is not essential to their use. For the sake of completeness, however, this theory is briefly reviewed herein. For the convenience of the reader, the report is presented under three main headings. The theory is found in the section entitled "Analysis." The validity of the theory and the accuracy of the curves is confirmed by comparison with experimental data obtained from references 3 and 4 in the section entitled "Comparison of Theoretical Results with Experimental Data." The use of the curves is illustrated by a typical example in the section entitled "Example of Use of Curves."

SYMBOLS

A	cross-sectional area of duct or radiator tube, square feet
a	velocity of sound in air, feet per second
c_f	skin-friction coefficient $\left(D_f/q_{r_2}S\right)$
C_{D_f}	mean skin-friction drag coefficient of radiator tube $\left(D_f/q_{r_2}A_{r_2}\right)$
c_p	specific heat at constant pressure (for air, 0.24 Btu/lb/°F)
D_f	drag force due to skin friction in a radiator tube
d	radiator-tube diameter, feet
g	acceleration of gravity, feet per second per second
H	heat added in radiator, Btu per second
h	total pressure, pounds per square foot
Δh	total-pressure loss, pounds per square foot
L	radiator-tube length, feet
M	Mach number (v/a)
m	mass-flow rate, slugs per second
m_{cr}	mass-flow rate at which sonic velocity is attained at tube entrance $\left(\frac{L}{d} = 0\right)$
p	static pressure, pounds per square foot
Δp	static-pressure decrease, pounds per square foot
q	dynamic pressure, pounds per square foot $\left(\frac{1}{2}\rho v^2\right)$

[redacted]

R Reynolds number $\left(\frac{\rho v d}{\mu} \text{ or } \frac{md}{A_{r_2}\mu}\right)$

S area of inside surface of radiator tube, square feet

T air temperature, °F absolute

ΔT air temperature rise, °F

v velocity in radiator tube or in duct, feet per second

ρ density, slugs per cubic foot

F_c compressibility factor $\left(1 + \frac{M^2}{4} + \frac{M^4}{40} + \frac{M^6}{1600} \cdots\right)$

μ viscosity of air, pound-seconds per square foot

Subscripts (see fig. 1):

2 station in duct ahead of radiator

3 station in duct behind radiator

f friction component

i low speed, incompressible-flow condition

r_2 within radiator at tube entrances

r_3 within radiator at tube exits

ANALYSIS

Derivation of Equation Relating Pressure Drops for Compressible and Incompressible Flow

For the purpose of the present analysis the pressure drop across the radiator is taken as the difference between the total pressure at a station just ahead of the front face of the radiator and the static pressure at the tube exits. A diagram of the flow system across the radiator is shown in figure 1. The station designations used in this figure were taken from reference 1. The pressure drop across the radiator for this system is

[redacted]

defined by the equation

$$\Delta p = h_2 - p_{r_3}$$

It will be shown subsequently herein that the results of the analysis can be applied to other definitions of the pressure drop, such as $p_2 - p_3$, $p_2 - p_{r_3}$, or $h_2 - h_3$.

The pressure drop can be conveniently divided into two components: the pressure drop due to acceleration of the air into the tube entrance and the pressure drop within the tube due to friction and momentum change. From equation 13 of reference 1, Δp may be expressed as the sum of these two components:

$$\Delta p = \left[q_{r_2} F_{c_{r_2}} \right] + \left[\frac{D_f}{A_{r_2}} + 2 q_{r_2} \left(\frac{\rho_{r_2}}{\rho_{r_3}} - 1 \right) \right] \qquad (1)$$

This equation can be evaluated with the aid of data given in references 1 and 5, but the process is not simple. The problem can be simplified by assuming that the pressure drop for cold incompressible-flow conditions, herein designated Δp_i, is known from basic test data for the radiator. The value of Δp for operating conditions can then be obtained if the ratio $\Delta p/\Delta p_i$ is evaluated. From equation (1), for the incompressible unheated condition $\left(F_c = 1, \frac{\rho_{r_2}}{\rho_{r_3}} = 1.0 \right)$, the calculated value of Δp_i is simply

$$\Delta p_i = q_{r_2} + q_{r_2} \left(\frac{D_{f_i}}{q_{r_2} A_{r_2}} \right) \qquad (2)$$

More specifically, since $q_{r_2} = \frac{1}{2\rho_2} \left(\frac{m}{A_{r_2}} \right)^2$ in incompressible flow and if $\frac{D_{f_i}}{q_{r_2} A_{r_2}}$ is replaced by $C_{D_{f_i}}$,

$$\Delta p_i = \frac{1}{2\rho_2} \left(\frac{m}{A_{r_2}} \right)^2 \left(1 + C_{D_{f_i}} \right) \qquad (2a)$$

[redacted]

An approximate application of equation (2a) that is in general use for estimating radiator pressure drops for conditions other than the test condition is

$$\Delta p = \Delta p_{test} \frac{\rho_{2_{test}}}{\rho_2}$$

The "test" pressure drop is measured with the mass flow m required for the design heat dissipation. This formula obviously neglects both Reynolds number effects (changes in $C_{D_{f_i}}$) and compressibility effects, both of which are too large to be neglected in many present-day applications.

It is convenient at this point to list the equations for evaluating Δp_i for all usable definitions of the radiator pressure drop. From equation (2) or (2a),

$$\left(\frac{h_2 - p_{r_3}}{q_{r_2}}\right)_i = 1 + C_{D_{f_i}} \tag{2b}$$

Similarly, since $p_2 = h_2 - q_2$ and $q_2 = q_{r_2}\left(\frac{A_{r_2}}{A_2}\right)^2$,

$$\left(\frac{p_2 - p_{r_3}}{q_{r_2}}\right)_i = 1 + C_{D_{f_i}} - \left(\frac{A_{r_2}}{A_2}\right)^2 \tag{2c}$$

In order to evaluate $\left(\frac{p_2 - p_3}{q_{r_2}}\right)_i$ an assumption must be made as to the location of station 3. It is assumed that this station is far enough behind the radiator for the velocity distribution across the duct to be uniform. Then, from equation 12 of reference 1, for incompressible flow,

$$\left(\frac{p_3 - p_{r_3}}{q_{r_2}}\right)_i = 2\left[\frac{A_{r_2}}{A_3} - \left(\frac{A_{r_2}}{A_3}\right)^2\right]$$

[redacted]

whence,

$$\left(\frac{p_2 - p_3}{q_{r_2}}\right)_i = 1 + C_{D_{f_i}} - \left(\frac{A_{r_2}}{A_2}\right)^2 - 2\left[\frac{A_{r_2}}{A_3} - \left(\frac{A_{r_2}}{A_3}\right)^2\right] \quad (2d)$$

The solution for incompressible flow,

$$h_2 - h_3 = p_2 - p_3 + q_2 - q_3$$

or

$$\left(\frac{h_2 - h_3}{q_{r_2}}\right)_i = \left(\frac{p_2 - p_3}{q_{r_2}}\right)_i + \left(\frac{A_{r_2}}{A_2}\right)^2 - \left(\frac{A_{r_2}}{A_3}\right)^2$$

is used to evaluate $\left(\frac{h_2 - h_3}{q_{r_2}}\right)_i$ by use of equation (2d) as

$$\left(\frac{h_2 - h_3}{q_{r_2}}\right)_i = 1 + C_{D_{f_i}} - 2\frac{A_{r_2}}{A_3} + \left(\frac{A_{r_2}}{A_3}\right)^2 \quad (2e)$$

As discussed in reference 1, the quantity $D_{f_i}/q_{r_2}A_{r_2}$ or $C_{D_{f_i}}$ is a drag coefficient. The value of this basic friction factor depends on the skin-friction coefficient and on the tube length-diameter ratio. From the definition of c_f,

$$C_{D_{f_i}} = \frac{D_{f_i}}{q_{r_2}A_{r_2}} = 4c_f\left(\frac{L}{d}\right)$$

The skin-friction coefficient c_f for a given tube depends only on the Reynolds number (references 3 and 4). The addition of heat within a tube has little effect on the local Reynolds number because the quantity ρv remains constant along the tube and, in usual cases, there is little change in viscosity. Figure 2, which is based on

[redacted]

the relations presented in reference 5, allows c_f and C_{Df_i} to be obtained for any tube L/d ratio for a wide range of Reynolds number or mass-flow rate. As indicated in figure 2, the Reynolds number may be evaluated directly from the mass-flow rate, the area, and the viscosity. For usual applications the viscosity at station 2 may be used instead of the viscosity at station r_2 with negligible error in the resulting pressure-drop evaluation.

The ratio of equation (1) to equation (2) can be expressed as

$$\frac{\Delta p/q_{r_2}}{\left(\Delta p/q_{r_2}\right)_i} = \frac{1}{1 + C_{Df_i}} \left[F c_{r_2} + \left(\frac{C_{Df}}{C_{Df_i}}\right) C_{Df_i} + 2\left(\frac{\rho_{r_2}}{\rho_{r_3}} - 1\right)\right]$$

Now

$$\frac{q_{r_2}}{q_{r_{2_i}}} = \frac{\frac{1}{2\rho_{r_2}}\left(\frac{m}{A_{r_2}}\right)^2}{\frac{1}{2\rho_2}\left(\frac{m}{A_{r_2}}\right)^2}$$

From reference 1, if q_2 is small in comparison with q_{r_2},

$$\frac{\rho_2}{\rho_{r_2}} = \left(1 + 0.2M_{r_2}{}^2\right)^{2.5}$$

Therefore,

$$\frac{\Delta p}{\Delta p_i} = \frac{\left(1 + 0.2M_{r_2}{}^2\right)^{2.5}}{1 + C_{Df_i}} \left[F c_{r_2} + \left(\frac{C_{Df}}{C_{Df_i}}\right) C_{Df_i} + 2\left(\frac{\rho_{r_2}}{\rho_{r_3}} - 1\right)\right] \quad (3)$$

Evaluation of Equation (3)

The method of evaluation of the terms in equation (3) for any combination of the known conditions ahead of the radiator, the mass-flow rate, and the heat-input rate will now be discussed.

[redacted]

The Mach number at the tube entrance M_{r_2}, which appears in equation (3), depends only on the known mass-flow rate, the known temperature and pressure at station 2, and the leak area through the radiator. From figure 3, M_{r_2} can be obtained directly for any combination of these basic conditions.

The terms C_{D_f}, $C_{D_{f_i}}$, and ρ_{r_2}/ρ_{r_3} in equation (3) are interdependent. The friction drag coefficient C_{D_f} for the actual operating condition is greater than $C_{D_{f_i}}$, except when the tube flow is cooled appreciably, as in the case of charge-air flow through intercoolers. The ratio $C_{D_f}/C_{D_{f_i}}$ is dependent on the values of M_{r_2} and ρ_{r_2}/ρ_{r_3}. These values govern the increase in dynamic pressure along the tube and hence determine the drag force due to skin friction D_f under actual operating conditions. In reference 1, an approximate empirical relation was assumed, as follows:

$$\frac{C_{D_f}}{C_{D_{f_i}}} = \frac{1}{2}\left(1 + \frac{\rho_{r_2}}{\rho_{r_3}}\right)$$

This relation has been found to be inaccurate except for values of ρ_{r_2}/ρ_{r_3} near unity. An exact evaluation of $C_{D_f}/C_{D_{f_i}}$ has been made for unheated tubes with the aid of reference 6. Equation 12 of reference 6 gives the following relation between $C_{D_{f_i}}$, M_{r_2}, and ρ_{r_2}/ρ_{r_3}, obtained from a solution of the differential

[redacted]

equation of the unheated flow through a constant-area tube:

$$C_{D_{f_i}} = \frac{1}{7}\left(1 + \frac{5}{M_{r_2}^2}\right)\left[1 - \left(\frac{\rho_{r_3}}{\rho_{r_2}}\right)^2\right] + \frac{6}{7}\log_e\left(\frac{\rho_{r_3}}{\rho_{r_2}}\right)^2 \quad (4)$$

From equation (10) of reference 1 the corresponding relation for C_{D_f}, based on considerations of continuity and of momentum and energy changes between the entrance and exit of the tube, is

$$C_{D_f} = \frac{\frac{\rho_{r_2}}{\rho_{r_3}} - 1 - 0.2M_{r_2}^2\left[1 - \left(\frac{\rho_{r_2}}{\rho_{r_3}}\right)^2 + 7.0\,\frac{\rho_{r_2}}{\rho_{r_3}}\left(\frac{\rho_{r_2}}{\rho_{r_3}} - 1\right)\right]}{0.7M_{r_2}^2\,\frac{\rho_{r_2}}{\rho_{r_3}}} \quad (5)$$

The ratio of equation (5) to equation (4) has been evaluated for the complete range of density-ratio values corresponding to a number of constant values of M_{r_2} and the results are plotted in figure 4.

The procedure then used in the evaluation of C_{D_f} and ρ_{r_2}/ρ_{r_3} with the aid of figure 4, for given values of $C_{D_{f_i}}$ and M_{r_2}, was as follows:

(1) On the assumption that $C_{D_f} \approx C_{D_{f_i}}$, equation 5 was used to obtain an approximate value of ρ_{r_2}/ρ_{r_3}. Figure 5(a) of reference 1 is a solution of equation 5.

[redacted]

(2) With this value of ρ_{r_2}/ρ_{r_3}, $C_{D_f}/C_{D_{f_i}}$ was determined from figure 4 and a second approximation for C_{D_f} was thus obtained.

(3) This more exact value of C_{D_f} was used and the procedure was repeated to obtain a third approximation for C_{D_f} and ρ_{r_2}/ρ_{r_3}.

The values determined from the third approximation were generally found to have the desired accuracy.

For unheated tubes all the quantities involved in the pressure-drop ratio (equation (3)) have been shown to be functions of only the two fundamental variables $C_{D_{f_i}}$ and M_{r_2}. The variable $C_{D_{f_i}}$ depends on the tube dimensions and Reynolds number, and the variable M_{r_2} depends on the mass flow and state of the air ahead of the radiator. Both variables can be simply evaluated for a given installation, as previously explained, for the particular design conditions under consideration. Equation 3 has been evaluated for a range of these parameters and the results are plotted in figure 5. Figure 5(a) shows the pressure-drop ratio plotted against M_{r_2} for unheated radiator tubes of various $C_{D_{f_i}}$ values.

When heat is added to the tubes, the density ratio ρ_{r_2}/ρ_{r_3} is increased and the drag coefficient C_{D_f} is correspondingly increased for a given mass flow. In the evaluation of C_{D_f} for the heated condition, the ratio $C_{D_f}/C_{D_{f_i}}$ from figure 4 was assumed to be the same, at a given ρ_{r_2}/ρ_{r_3} and M_{r_3}, as for the unheated condition for which figure 4 is exact. This assumption is believed justified for practical purposes. If heat were added uniformly at low speed, linear reduction in density due to heating would occur along the tube. For a given value of ρ_{r_2}/ρ_{r_3}, the ratio $C_{D_f}/C_{D_{f_i}}$ would be greater for a heated tube than for an unheated tube because of the nonlinearity of the density variation for

[redacted]

the unheated tube at the higher Mach number at which the unheated tube would have to operate to give the same ρ_{r_2}/ρ_{r_3} value as the heated tube. Results based on the assumption that the drag-coefficient ratio is the same for heated or unheated flow will thus tend to underestimate the required pressure drop when heat is added. The probable error will be seen to be small for usual operating conditions because the pressure-drop ratio $\Delta p/\Delta p_1$ is not critically dependent on the value of C_{D_f} for these conditions. The tube Mach number for these conditions is generally well below the critical, and the density variation along unheated tubes then approaches linearity. The assumption made in calculating C_{D_f} for the heated condition would therefore not be expected to result in appreciable error when the entrance Mach number is well below the critical.

The relationship among C_{D_f}, M_{r_2}, and ρ_{r_2}/ρ_{r_3} for heated tubes is given in figure 5 of reference 1 for constant values of the heat-input parameter $\frac{H}{c_p g m T_{r_2}}$. This figure was used with figure 4 as described for the unheated condition to obtain corresponding values of $C_{D_{f_1}}$, C_{D_f}, and ρ_{r_2}/ρ_{r_3} for constant values of $\frac{H}{c_p g m T_{r_2}}$. Values of $\Delta p/\Delta p_1$ were then computed from equation 3 and are shown in figures 5(b) to 5(g). Each part of figure 5 corresponds to a constant value of $\frac{H}{c_p g m T_{r_2}}$. As discussed in reference 1, for the incompressible condition,

$$\frac{H}{c_p g m T_{r_2}} = \frac{\Delta T}{T_{r_2}}$$

Interpolation will be required to determine $\Delta p/\Delta p_1$ for values of the heat-input parameter intermediate to those for which the curves were derived. The heat-input parameter may be evaluated from the following relation derived on the assumption that v_2 is small in comparison with v_{r_2}:

$$\frac{H}{c_p g m T_{r_2}} = 0.1293 \left(\frac{H}{m T_2}\right)\left(1 + 0.2 M_{r_2}^2\right) \qquad (6)$$

[redacted]

The results shown in figure 5 indicate that appreciable compressibility effects on the radiator pressure drop exist even at relatively low entrance Mach numbers, particularly for tubes of large values of L/d (large values of C_{Df_i}) and for installations in which high rates of heating are used. The limiting values shown on the curves correspond to the attainment of sonic velocity at the tube exits. No increase in mass flow through the tubes can be effected by lowering the exit pressure below the limiting value corresponding to sonic exit velocity. It is interesting to note that this limiting condition occurs at $M_{r_2} = 0.48$ for an unheated radiator tube of $C_{Df_i} = 1.2$ (fig. 5(a)), which corresponds to a 0.196-inch diameter tube with a typical value of L/d of about 60 for standard conditions ahead of the radiator (fig. 2).

The curves of figures 5(b) to 5(g) include the effects of both heating and Mach number; that is, the figures as given show the net effect of compressibility (density change) on the pressure drop. If separation of the two effects is desired, the Mach number effect alone can be determined from figure 5(a) for comparison with the net effect for the heated condition.

General Application of Equation (3)

Test data for radiators are frequently given in terms of $p_2 - p_3$, $p_2 - p_{r_3}$, or $h_2 - h_3$, rather than in terms of $h_2 - p_{r_3}$, which was used in the present analysis. The absolute values of the pressure drop vary, depending on the definition, by 5 to 15 percent in usual cases. The ratio $\Delta p/\Delta p_i$, however, can readily be shown to be essentially the same for all the definitions of the pressure drop. Figure 5 may therefore be used to evaluate the compressibility effects for other radiator pressure-drop definitions as well as for $h_2 - p_{r_3}$.

Once the ratio $\Delta p/\Delta p_i$ is obtained from figure 5 for the design values of C_{Df_i}, M_{r_2}, and $\frac{H}{c_p g m T_{r_2}}$, the pressure drop for compressible flow may be obtained

[redacted]

from an evaluation of the pressure drop for incompressible flow. For this purpose, use of test data for the unheated radiator obtained with moderate rates of air flow (low Mach numbers) is generally desirable. This value of the pressure drop is then corrected to the design mass-flow and Reynolds number conditions in the usual manner without allowance for compressibility effects. With Δp_1 so determined, the correct pressure drop is computed from

$$\Delta p = \left(\frac{\Delta p}{\Delta p_1}\right) \Delta p_1 \qquad (7)$$

COMPARISON OF THEORETICAL RESULTS WITH EXPERIMENTAL DATA

A limited amount of test data on the pressure drop in unheated tubes at Mach numbers up to the critical is available from references 3 and 4. Similar data for heated tubes are not available. The available data will be analyzed and put into such form that direct comparison can be made with the theoretical results shown by the curves of figure 5(a).

Experimental data from reference 3.- Reference 3 presents pressure-drop data for cylindrical tubes of circular section with rounded entries. Air was admitted from a large reservoir at atmospheric pressure. The pressure at the exit was progressively reduced until the limiting flow condition was attained. The measured mass-flow rate was expressed nondimensionally as m/m_{cr}. This term is the ratio of the actual mass flow through the tube to the mass flow that would exist if sonic velocity were attained at the tube entrance. This parameter may be expressed in terms of the entrance Mach number as

$$\frac{m}{m_{cr}} = \frac{1.728\, M_{r_2}}{\left(1 + 0.20 M_{r_2}^{\,2}\right)^3}$$

Pressure data from reference 3 for 20-millimeter-diameter tubes with $L/d = 10$ and $L/d = 60$ are given in table I. Values of M_{r_2} corresponding to equally spaced values of $\frac{m}{m_{cr}}$, for which the pressure data were taken from reference 3,

[redacted]

are listed as column 2 of table I. The maximum values of m/m_{cr} and M_{r_2} shown in table I were the highest that could be attained in the tests regardless of the outlet pressure and represent the condition at which sonic velocity was reached at the tube exits.

In computing the values of $\Delta p/\Delta p_i$ from the experimental data, equation 2(a) was used; that is

$$\Delta p_i \propto m^2 \propto \left(\frac{m}{m_{cr}}\right)^2$$

and, since p_2 was a constant in the tests of reference 3,

$$\frac{\Delta p}{\Delta p_i} = \frac{K \frac{\Delta p}{p_2}}{\left(m/m_{cr}\right)^2}$$

The experimental values of columns (1) and (3) were used to determine the value in column (4) of table I. The value of K was then chosen to make the experimental value of $\Delta p/\Delta p_i$ at the lowest test speed $\left(M_{r_2} = 0.240\right)$ agree with the theoretical value obtained from figure 5(a) for this low speed. The resulting experimental values of $\Delta p/\Delta p_i$ are shown in column 5. The theoretical values of $\Delta p/\Delta p_i$ shown in column 7 for comparison with these experimental results were taken from figure 5(a) for the values of M_{r_2} of column 2 and for values of $C_{D_{f_i}}$ computed from figure 2 for 20-millimeter-diameter tubes with $L/d = 10$ and $L/d = 60$. Standard atmospheric entrance conditions and mass-flow values corresponding to m/m_{cr} are assumed. The results shown in columns 5 and 7 are plotted against M_{r_2} in figure 6.

The agreement between the pressure-drop ratios for the theory presented and for experiment will be seen to be unusually close. The limiting flow condition, in which sonic velocity was attained at the tube exits, was also accurately predicted by the theory.

Experimental data from reference 4.- The data given in reference 4 were obtained with a cylindrical pipe 0.375 inches in diameter and ten feet long. Extremely high pressure drops were required to induce high-speed flow through the tube because of its unusually high L/d ratio of 320. Inlet pressures of several atmospheres were used. The tests consisted of measurements of pressure distribution along the pipe for four combinations of inlet pressure and outlet pressure. The results of the tests were analyzed in reference 4 to determine values of the effective friction coefficient c_f. The value of c_f was found to be independent of the Mach number and to depend on only the Reynolds number, as assumed in the present report; furthermore, the values of Reynolds number and c_f were virtually the same at all stations along the tube, as was assumed in the present analysis. Values of $C_{D_{f_i}}$ from the test data agreed with theoretical values from figure 2 to within 4 percent.

In evaluating experimental values of the over-all pressure-drop ratio $\Delta p/\Delta p_i$, Δp_i was calculated from equation (2a) as

$$\Delta p_i = \left(\frac{1}{2\rho_2}\right)\left(\frac{m}{A_{r_2}}\right)^2\left(1 + 4c_f\frac{L}{d}\right)$$

The basic data required for evaluation of Δp_i from this form of equation (2) are listed in reference 3. The over-all pressure drop Δp and the Mach number M_{r_2} were obtained directly from tabulations of the pressures and the Mach number in reference 3. A comparison of the test values of $\Delta p/\Delta p_i$ with theoretical values taken from figure 5(a) is shown in the following table:

Experimental					Theoretical
p_2 (lb/sq ft)	M_{r_2}	$C_{D_{f_i}}$	Δp (lb/sq ft)	$\frac{\Delta p}{\Delta p_i}$	$\frac{\Delta p}{\Delta p_i}$
4,146	0.270	5.84	2,073	1.47	1.51
7,422	.308	4.94	5,414	[a]2.02	[a]2.09
16,179	.327	4.13	11,891	[a]2.18	[a]2.11
17,607	.297	4.12	7,555	1.51	1.49

[a]Sonic velocity attained at tube exit.

[redacted]

Good agreement between theory and experiment is shown. The accuracy of the theoretical curves of figure 5 has been verified for the conditions of extremely high inlet pressures, as well as for the more usual conditions (atmospheric inlet pressure) existing for the tests of reference 3, which are shown in table I and figure 6.

As a matter of further interest, a check on the validity of the present theory may be made by computing the pressure distribution along the tube and comparing the results with the experimental data. These calculations were made by use of the present theoretical method, in which the pressure drops were computed for tubes of the same diameter (3/8 inch) as the test model but of lengths varying from 1 to 10 feet. The computed pressure drop for a tube 3 feet long, for example, was compared with the measured pressure drop from the tube entrance to the 3-foot station. The theoretical pressures obtained from these computations are compared with experimental values in figure 7. Reasonably good agreement will be noted for all four test conditions.

A principal assumption of the present theory was that the velocity profile across the tube section was uniform at all stations along the tube. The results of the comparisons in table I and in figures 6 and 7 indicate this assumption to be fully justified. In the analysis of reference 7, in which account was taken of the velocity-profile shape, a similar conclusion was obtained theoretically.

EXAMPLE OF USE OF CURVES

The use of the curves will be illustrated by calculating the pressure drop for an oil radiator for typical operating conditions. The dimensions of the radiator are as follows:

Diameter, inches	12
Duct diameter, inches	12
Tube length, inches	12
Tube diameter (inside), inches	0.196
Tube diameter (outside), inches	0.210
Number of tubes	1900
Free-flow area, A_{r_2}, square feet	0.397
Duct area, A_2 and A_3, square feet	0.785

[redacted]

Basic radiator performance data.- Performance data for the radiator are shown in figure 8 in the form that is most generally used. The air pressure-drop data given in curves of this type are frequently of limited value because the pressure drop is not adequately defined and because the test conditions under which it was measured are not stated. As previously discussed, the pressure drop may be measured by any one of at least four methods. It is obviously necessary to state which method was used. Pressure-drop data for the unheated radiator are valuable because they can be conveniently corrected to actual operating conditions by analytical means. Data for a specific heated condition are inconvenient to use because they must first be corrected to the unheated condition. The very wide variation of the heat-input parameter encountered in actual installations makes it unlikely that the test values of this parameter will coincide with the required design value.

Assumed operating conditions.- The following assumed operating conditions apply to a typical oil-cooler installation in an airplane flying in standard sea-level air at a speed of the order of 400 miles per hour:

Air temperature at station 2, °F	88
Air pressure at station 2, p_2, pounds per square foot, absolute	2554
Air density at station 2, ρ_2, slugs per cubic foot	0.00272
Average oil temperature, °F	200
Oil flow, pounds per minute	120
Heat rejection, H, Btu per second	75

The heat rejected per minute per hundred degrees temperature difference between the oil and the inlet-air stagnation temperature is

$$\frac{60 \times 75 \times 100}{200 - 88} = 4020 \text{ Btu per minute per } 100^\circ\text{F}$$

With this value, the weight flow of air required is found in figure 8 to be 462 pounds per minute. The mass flow is

$$m = \frac{462}{60 \times 32.2}$$

$$= 0.239 \text{ slugs per second}$$

[redacted]

The required mass flow will deviate slightly from this value if the tube Reynolds number varies from the test conditions of figure 8. On the basis of the proportionality relationship between the heat-transfer and skin-friction coefficients, the change in skin-friction coefficient with Reynolds number (fig. 2) may be used to estimate the corresponding change in heat-transfer coefficient and hence to determine the change in mass flow required. This effect is usually slight and, since only the mass-flow determination is involved, is considered to be outside the scope of the present report and will be neglected.

Calculation of friction drag coefficient, $C_{D_{f_i}}$.-

The tube Reynolds number is

$$R = \frac{md}{A_{r_2}\mu}$$

$$= \frac{0.239 \times \frac{0.196}{12}}{0.397 \times 3890 \times 10^{-10}}$$

$$= 25{,}300$$

From figure 2, for this value of Reynolds number and for $L/d = 61.2$,

$$c_f = 0.0057$$

and

$$C_{D_{f_i}} = 4 \times 61.2 \times 0.0057$$
$$= 1.40$$

Calculation of Mach number.- The use of the curves of figure 5 requires the Mach number M_{r_2} at the tube entrance. Figure 3 gives M_{r_2} directly in terms of the known flow conditions ahead of the radiator; thus,

[redacted]

$$\frac{m\sqrt{T_{r_2}}}{A_{r_2}p_2} = \frac{0.239 \times (460 + 89)^{0.5}}{0.397 \times 2540}$$

$$= 0.0554$$

With this value, the Mach number is found from figure 3 to be

$$M_{r_2} = 0.198$$

Calculation of heat-input parameter.- The rate of heat input is specified on the curves of figure 5 by the nondimensional parameter $H/c_p g m T_{r_2}$. This quantity is evaluated from equation (6) as

$$\frac{H}{c_p g m T_{r_2}} = 0.1293 \left(\frac{75}{0.239 \times 548}\right) \left[1 + 0.2(0.198)^2\right]$$

$$= 0.074$$

Compressibility effect.- The pressure-drop ratio $\Delta p/\Delta p_i$ is taken from figure 5 for $C_{D_{f_i}} = 1.40$, $M_{r_2} = 0.198$, and $\frac{H}{c_p g m T_{r_2}} = 0.074$. Interpolation between the curves of figure 5(b) and figure 5(c) is necessary because the heat-input parameter is intermediate between the values for these two parts of figure 5. The pressure-ratio value obtained is

$$\frac{\Delta p}{\Delta p_i} = 1.17$$

For this case, the effect of compressibility is to increase the pressure drop 17 percent above the value for incompressible flow. In order to compute the actual pressure drop Δp, Δp_i must first be obtained.

Calculation of Δp_i.- The basic incompressible-flow value of the pressure drop can be obtained from low-speed test data or from calculations based on the radiator-tube friction coefficients shown in figure 2. The method

[redacted]

involving the theoretical calculations requires the use of equation (2d) because the test pressure-drop data for the present example is in terms of $p_2 - p_3$. From equation (2d), therefore, since $A_2 = A_3$ and $\frac{A_{r_2}}{A_2} = 0.506$,

$$\left(\frac{\Delta p}{q_{r_2}}\right)_1 = \left(\frac{p_2 - p_3}{q_{r_2}}\right)_1$$

$$= 1 + 1.40 - (0.506)^2 - 2\left[0.506 - (0.506)^2\right]$$

$$= 1.64$$

This computed value of $\Delta p_1/q_{r_2}$ will now be compared with the value obtained from the test data of figure 8.

For a pressure drop of 5 inches of water, the flow may safely be considered incompressible. At this test condition the weight flow is 197 pounds per minute. Therefore,

$$m = \frac{197}{32.2 \times 60}$$

$$= 0.102 \text{ slugs per second}$$

and, for incompressible flow,

$$\left(q_{r_2}\right)_1 = \frac{1}{2\rho_2}\left(\frac{m}{A_{r_2}}\right)^2$$

$$= \frac{1}{2(0.002378)}\left(\frac{0.102}{0.397}\right)^2$$

$$= 13.9$$

whence, for $m = 0.102$,

$$\left(\frac{\Delta p}{q_{r_2}}\right)_1 = \frac{5 \times 5.21}{13.9}$$

$$= 1.87$$

[redacted]

This value is greater than the previously calculated value for $m = 0.239$ because of the lower tube Reynolds number at $\Delta p = 5$ inches of water ($m = 0.102$). The Reynolds number for this low mass flow is

$$R = \frac{md}{A_{r_2}\mu}$$

$$= \frac{0.102 \times \frac{0.196}{12}}{0.397 \times 3950 \times 10^{-10}}$$

$$= 10,600$$

The value of the tube friction-drag coefficient for this mass flow is, from figure 2,

$$\left(C_{D_{f_i}}\right)_m = 0.102 = \frac{4 \times 12 \times 0.0068}{0.196}$$

$$= 1.66$$

The value of $C_{D_{f_i}}$ for the design condition has been previously computed as 1.40. The correction to be applied to the low-speed test value of the pressure drop (see equation (2)) is $q_{r_2}(1.66 - 1.40)$; therefore,

$$\left(\frac{\Delta p}{q_{r_2}}\right)_i = 1.87 - (1.66 - 1.40)$$

$$= 1.61$$

This result, based on the test data, compares very satisfactorily with the value 1.64 previously computed from equation (2b) and equation (7).

The value of Δp_i for the design condition is

$$\Delta p_i = 1.64 \left(q_{r_2}\right)_i$$

[redacted]

$$\Delta p_i = 1.64 \times \frac{1}{2\rho_2}\left(\frac{m}{A_{r_2}}\right)^2$$

$$= 1.64 \times \frac{1}{2 \times 0.00272}\left(\frac{0.239}{0.397}\right)^2$$

$$= 110 \text{ pounds per square foot}$$

Calculation of Δp.- The value of the pressure drop corrected for compressibility is, finally,

$$\Delta p = \frac{\Delta p}{\Delta p_i} \times \Delta p_i$$

$$= 1.17 \times 110$$

$$= 129 \text{ pounds per square foot}$$

Altitude effect.- The calculations made in the illustrative example for standard sea-level conditions have been repeated for standard conditions at an altitude of 30,000 feet. The same heat rejection, rate of oil flow, oil temperature, and airplane speed were assumed for both cases. The results obtained in the two cases are compared in the following table:

Quantity	Sea level	30,000 feet
Air temperature, t_2, °F	88	-19
Air pressure, p_2, lb/sq ft	2540	795
Air density, ρ_2, slugs/cu ft	0.00270	0.00105
Heat rejection, Btu/min/100°F	4020	2055
Mass flow, slugs/sec	0.239	0.070
Reynolds number	25,300	8720
Friction coefficient, $C_{D_{f_i}}$	1.40	1.72
Mach number, M_{r_2}	0.198	0.165
Heat-input factor, $H/c_p g m T_{r_2}$	0.074	0.314
Pressure drop with compressibility neglected, Δp_i, lb/sq ft	110	29
Pressure drop corrected for compressibility, Δp, lb/sq ft	129	41
Compressibility correction, percent Δp_i	17	41

[redacted]

The compressibility effect is shown to increase from 17 percent at sea level to 41 percent at 30,000 feet for the typical oil-radiator installation assumed in the example. It is of interest to note that the oil-cooler tube Mach number is somewhat less at altitude than at sea level. A very large increase in the heat-input parameter occurs, however, because of the decrease in mass flow required and the heating effect therefore becomes very large.

Other types of cooler installation frequently require an increasing value of M_{r_2} with altitude. In the case of ethylene-glycol radiators, for example, the Mach number effect generally becomes very large at altitude and, in many cases, makes it impossible to obtain adequate cooling-air flow.

Summary of method.- The steps required in the use of the curves of figure 5 to obtain the corrected value of the pressure drop are summarized as follows:

(1) Determine the pressure, temperature, and density of the air ahead of the radiator and the heat to be dissipated.

(2) Obtain the required mass flow of cooling air from the usual heat-dissipation data for the radiator.

(3) Compute the Reynolds number of the tube flow and obtain the friction drag factor $C_{D_{f_i}}$ from figure 2.

(4) Obtain the Mach number of the tube flow M_{r_2} from figure 3.

(5) Evaluate the heat-input factor $H/c_p g m T_{r_2}$ by equation (6).

(6) From figure 5 with these values of $C_{D_{f_i}}$, M_{r_2}, and $H/c_p g m T_{r_2}$, obtain the pressure-drop ratio $\Delta p/\Delta p_i$.

(7) Compute Δp_i from equations (2) or obtain it from low-speed test data corrected to the design Reynolds number.

(8) Evaluate Δp by multiplying Δp_i by the pressure-drop ratio $\Delta p/\Delta p_i$.

[redacted]

CONCLUSIONS

Simple curves are presented by which the basic pressure-drop characteristics of unheated tubular radiators can be corrected to operating conditions in which the radiator is heated and in which the Mach number of the tube flow is of appreciable magnitude. The following conclusions are indicated:

1. The accuracy of the simple method presented for evaluating the compressibility effects is verified for unheated tubes for the complete range of attainable flow (tube exit Mach numbers from 0 to 1.0) by experimental data from two sources.

2. The effects of compressibility (density change) on the pressure drop required to provide a given mass flow of cooling air through a tubular radiator are shown to be of appreciable magnitude under present-day operating conditions. Calculations for a typical oil-cooler installation indicated that the compressibility effect increased the pressure drop by 17 percent at sea level and by 41 percent at an altitude of 30,000 feet.

Langley Memorial Aeronautical Laboratory
National Advisory Committee for Aeronautics
Langley Field, Va.

[redacted]

REFERENCES

1. Becker, John V., and Baals, Donald D.: The Aerodynamic Effects of Heat and Compressibility in the Internal Flow Systems of Aircraft. NACA ACR, Sept. 1942.

2. Wood, George P.: Use of Stagnation Temperature in Calculating Rate of Heat Transfer in Aircraft Heat Exchangers. NACA RB No. 3J30, 1943.

3. Frössel, W.: Flow in Smooth Straight Pipes at Velocities above and below Sound Velocity. NACA TM No. 844, 1938.

4. Keenan, Joseph H., and Neumann, Ernest P.: Measurements of Friction Coefficients in a Pipe for Subsonic and Supersonic Flow of Air. NACA ARR No. 3G13, 1943.

5. Brevoort, M. J., and Leifer, M.: Radiator Design and Installation. NACA ACR, May 1939.

6. Hawthorne, W. R.: Simplified Analysis of Frictional and Compressible Flow in Pipes. Note No. E.3929, R.A.E. (British), March 1942.

7. Young, A. D., and Winterbottom, N. E.: High Speed Flow in Smooth Cylindrical Pipes of Circular Section. Rep. No. Aero. 1785, R.A.E. (British), Nov. 1942.

[redacted]

TABLE I

ANALYSIS OF DATA FOR 20-MILLIMETER-DIAMETER TUBES FROM REFERENCE 3

Experimental					Theoretical	
$\frac{m}{m_{cr}}$	M_{r_2}	$\frac{\Delta p}{p_2}$	$\frac{\frac{\Delta p}{p_2}}{(m/m_{cr})^2}$	$\frac{\Delta p}{\Delta p_1}$	$C_{D_{f_1}}$	$\frac{\Delta p}{\Delta p_1}$
L/d = 10						
0.40	0.240	0.050	0.312	1.05	0.171	1.05
.45	.273	.065	.320	1.08	.166	1.07
.50	.307	.080	.320	1.08	.161	1.09
.55	.342	.100	.331	1.11	.158	1.11
.60	.378	.120	.334	1.12	.154	1.14
.65	.418	.145	.344	1.16	.151	1.17
.70	.458	.175	.357	1.20	.148	1.22
.75	.502	.210	.373	1.26	.146	1.27
.80	.553	.255	.399	1.34	.143	1.34
.85	.610	.315	.436	1.47	.141	1.45
.90	.678	.400	.493	1.66	.139	1.65
[a].93	.728	.550	.640	[a]2.16	.138	2.01
L/d = 60						
0.40	0.240	0.085	0.530	1.10	1.026	1.10
.45	.273	.110	.543	1.13	.996	1.13
.50	.307	.140	.560	1.17	.966	1.17
.55	.342	.175	.578	1.20	.948	1.22
.60	.378	.220	.612	1.27	.924	1.28
.65	.418	.275	.650	1.35	.906	1.36
.70	.458	.340	.694	1.45	.888	1.47
.75	.502	.460	.818	1.70	.876	1.73
[a].77	.522	.630	1.062	[a]2.22	.870	[a]2.20

[a]Sonic velocity attained at tube exit.

NATIONAL ADVISORY
COMMITTEE FOR AERONAUTICS

[redacted]

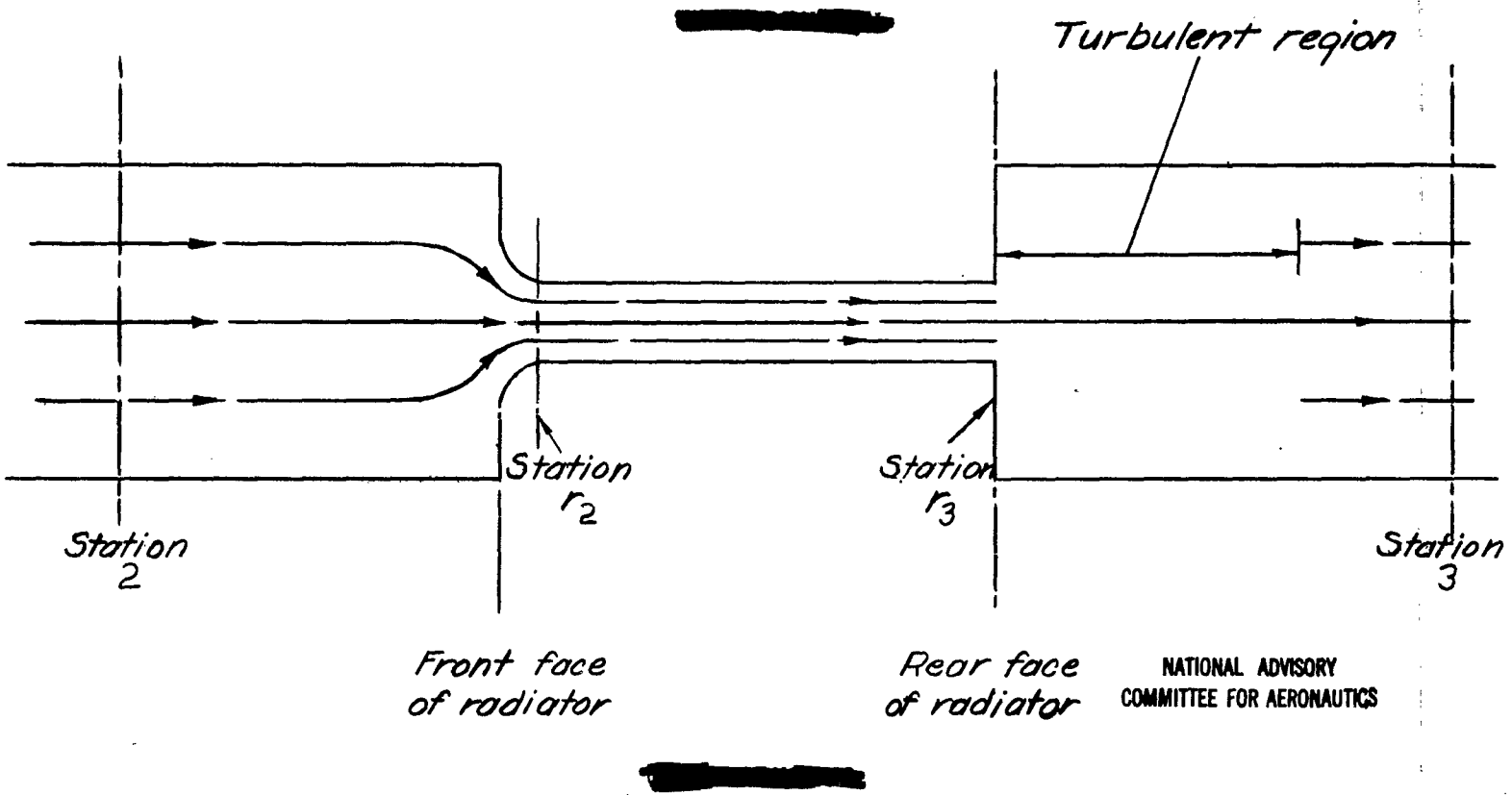

Figure 1 :- Diagram of assumed flow system.

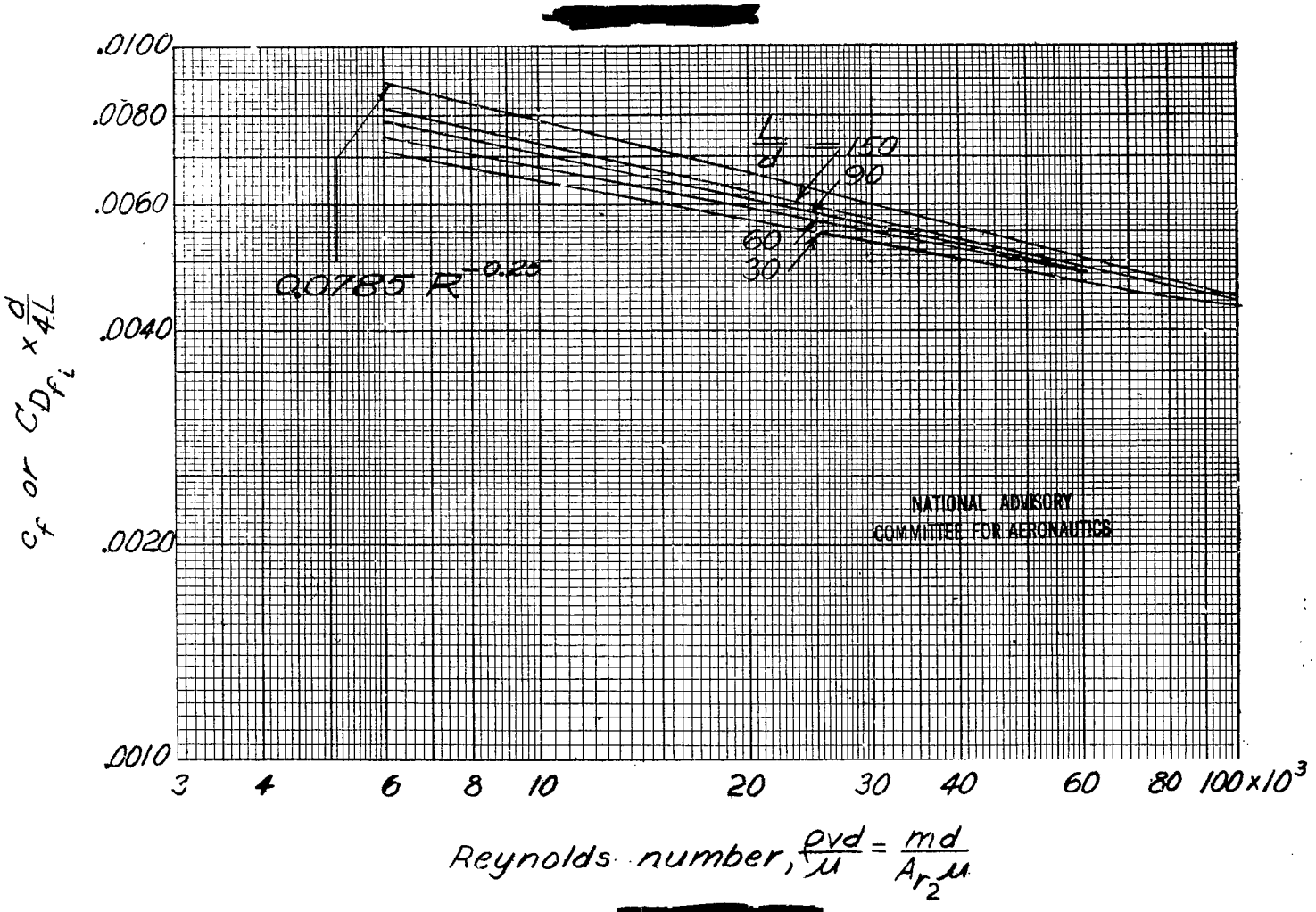

Figure 2.- Variation of tube friction coefficient with Reynolds number.

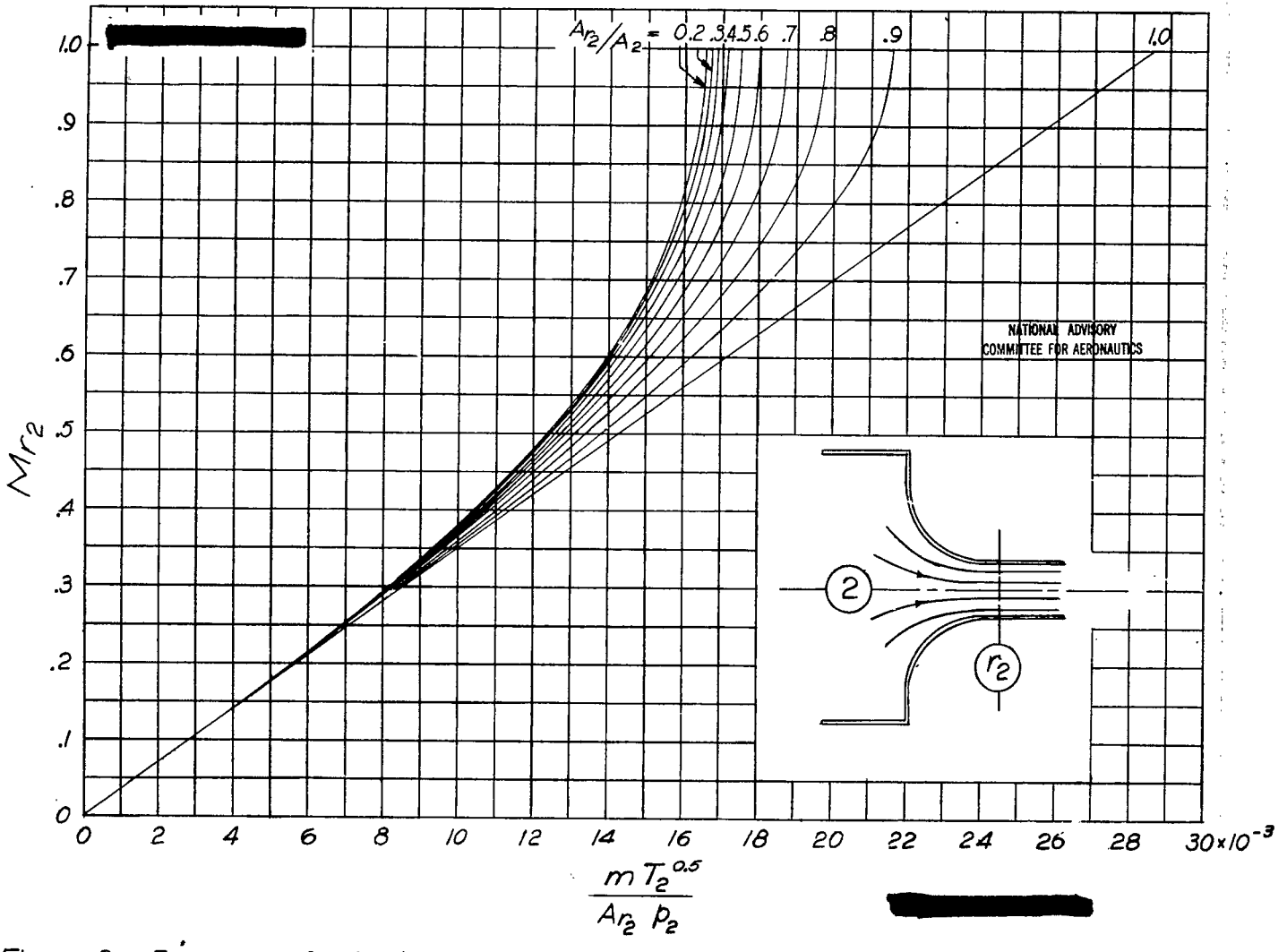

Figure 3.- Evaluation of M_{r_2} in terms of the mass flow and conditions at station 2.

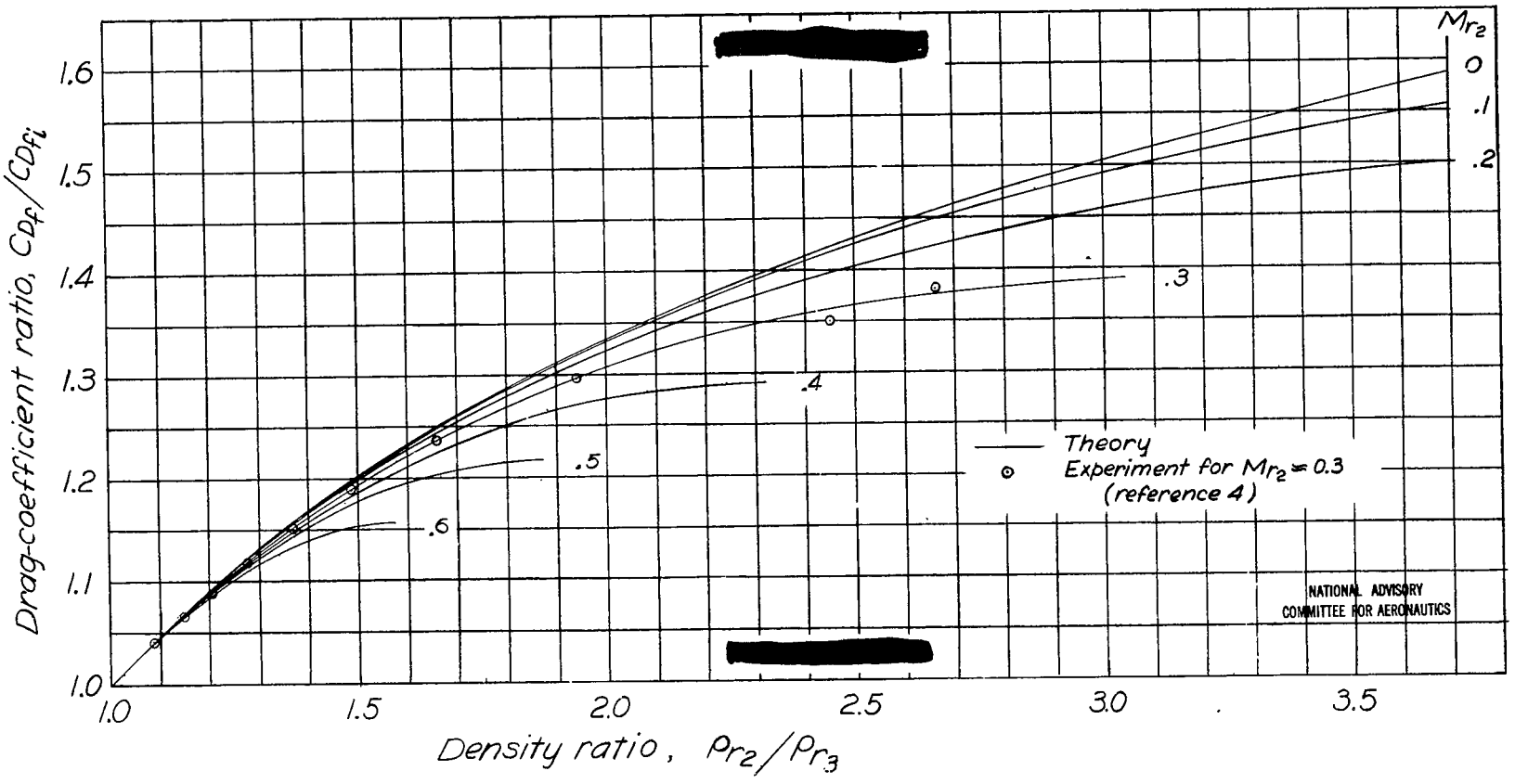

Figure 4.- Variation of drag-coefficient ratio with density ratio for various values of entrance Mach number.

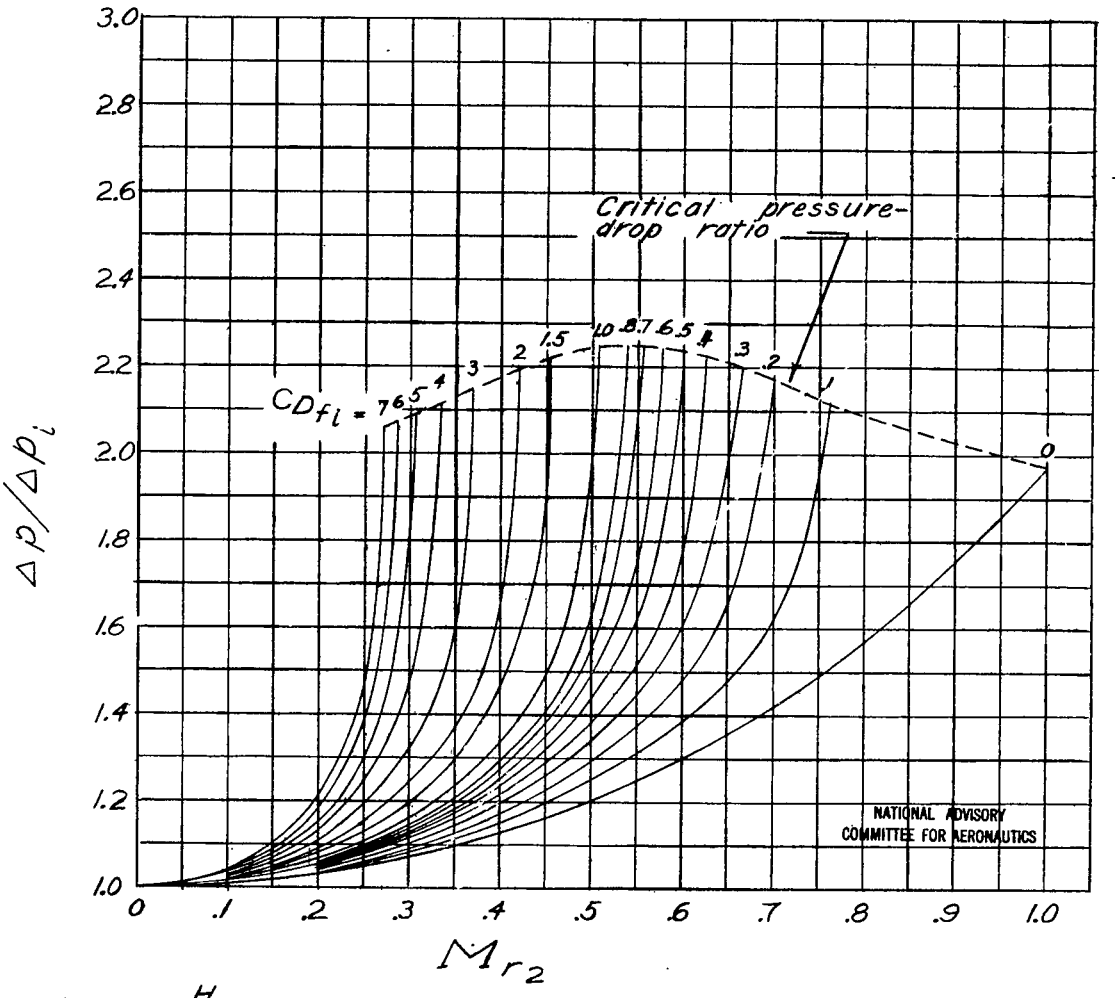

(a) $\frac{H}{c_p g m T_{r_2}} = 0.$ [redacted]

Figure 5.— Variation of static-pressure-drop ratio with Mach number.

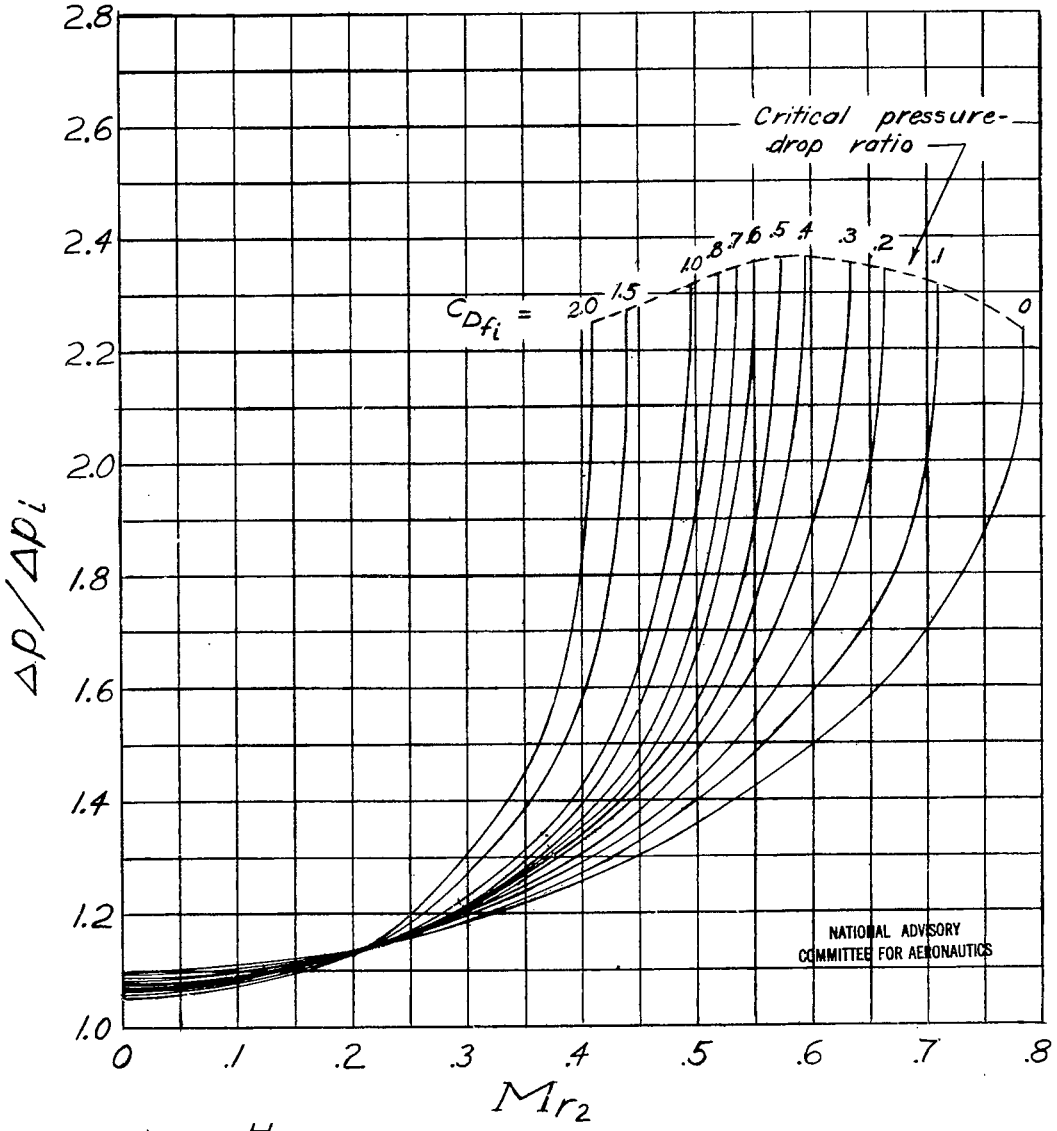

(b) $\frac{H}{c_p g m T_{r_2}} = 0.05.$ [redacted]

Figure 5.- Continued.

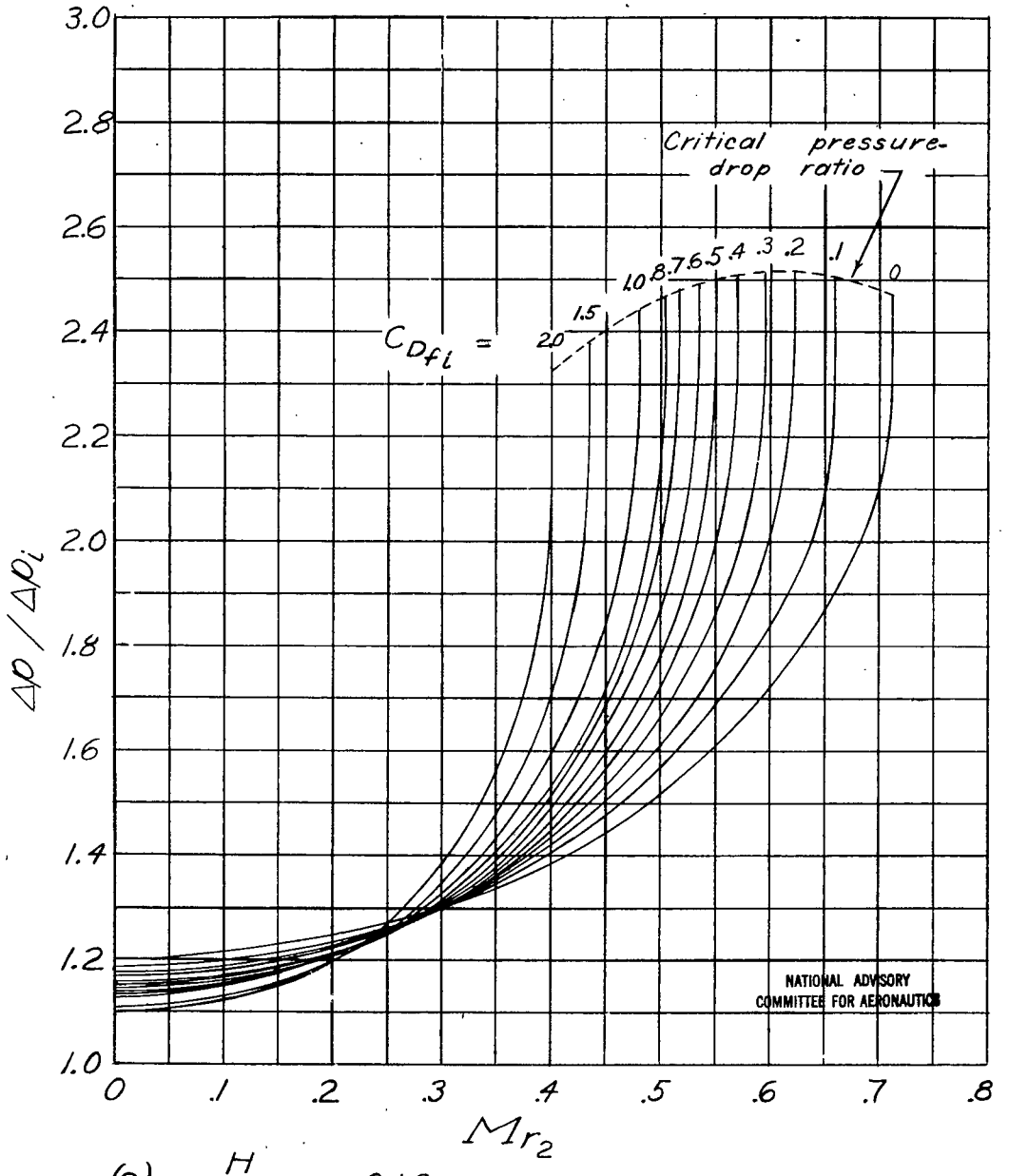

(c) $\frac{H}{c_p g m T_{r_2}} = 0.10.$ [redacted]

Figure 5. – Continued.

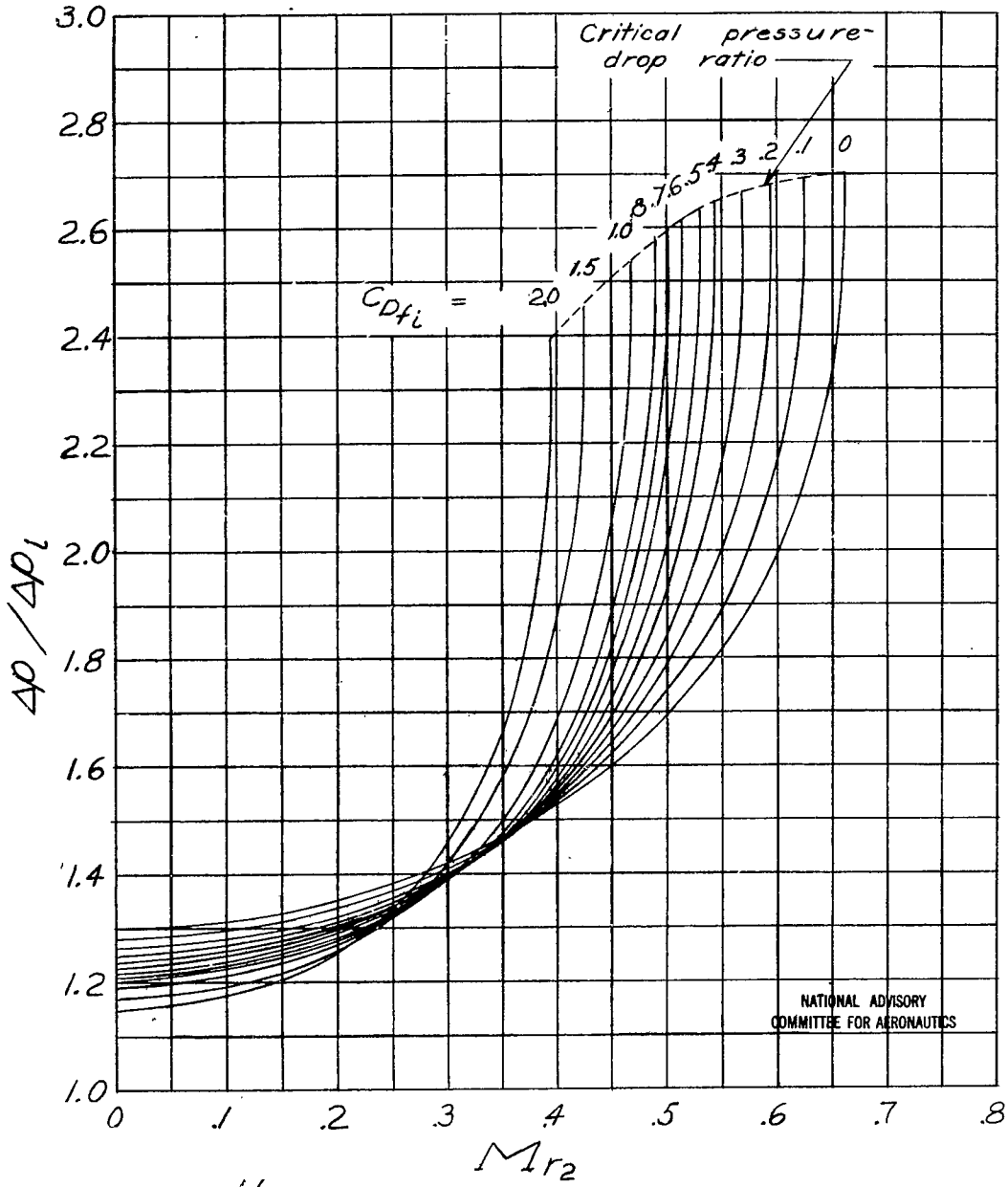

(d) $\frac{H}{c_p g m T_{r_2}} = 0.15.$ [redacted]

Figure 5.- Continued.

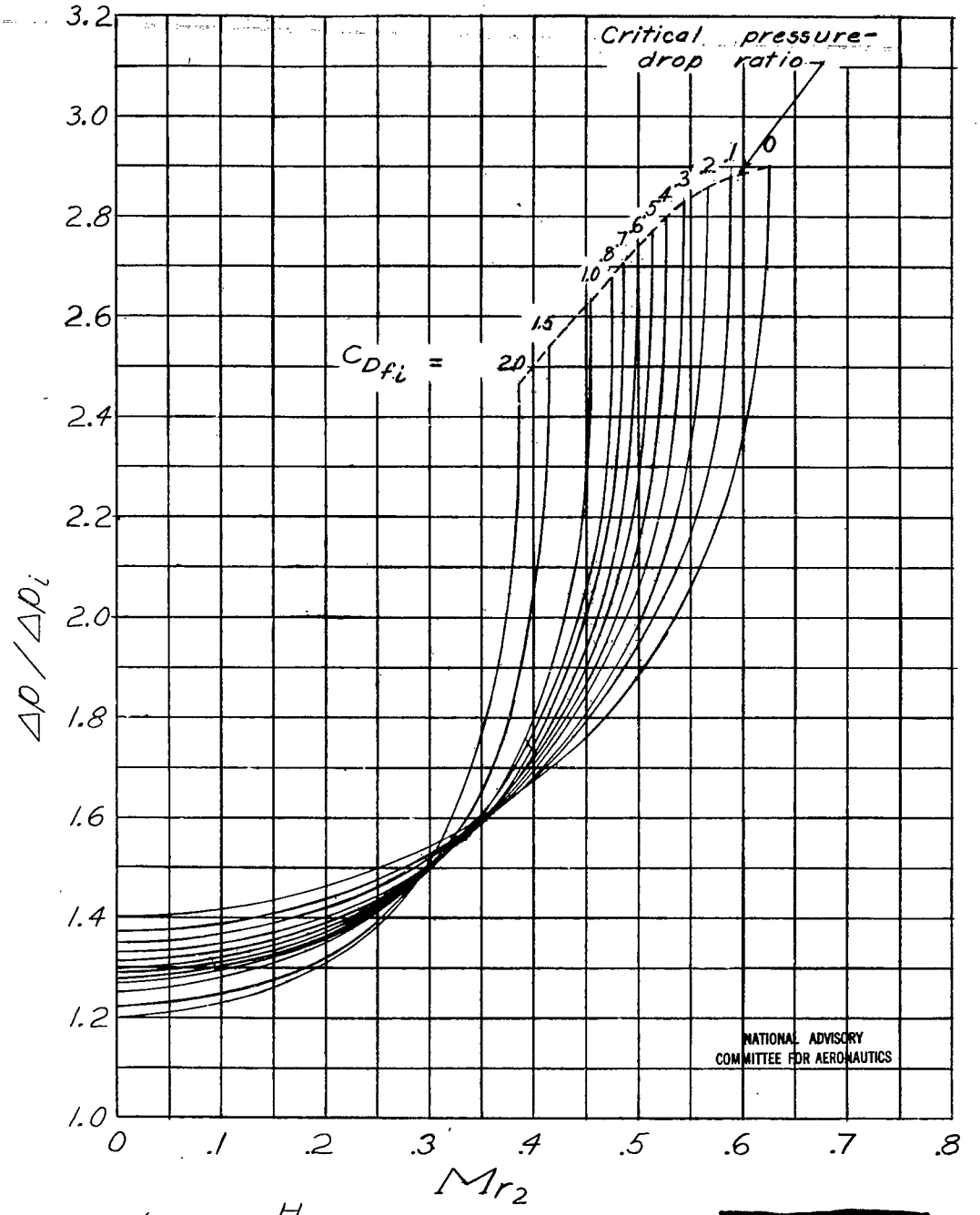

(e) $\frac{H}{c_p g m T_{r_2}} = 0.20.$

Figure 5.– Continued.

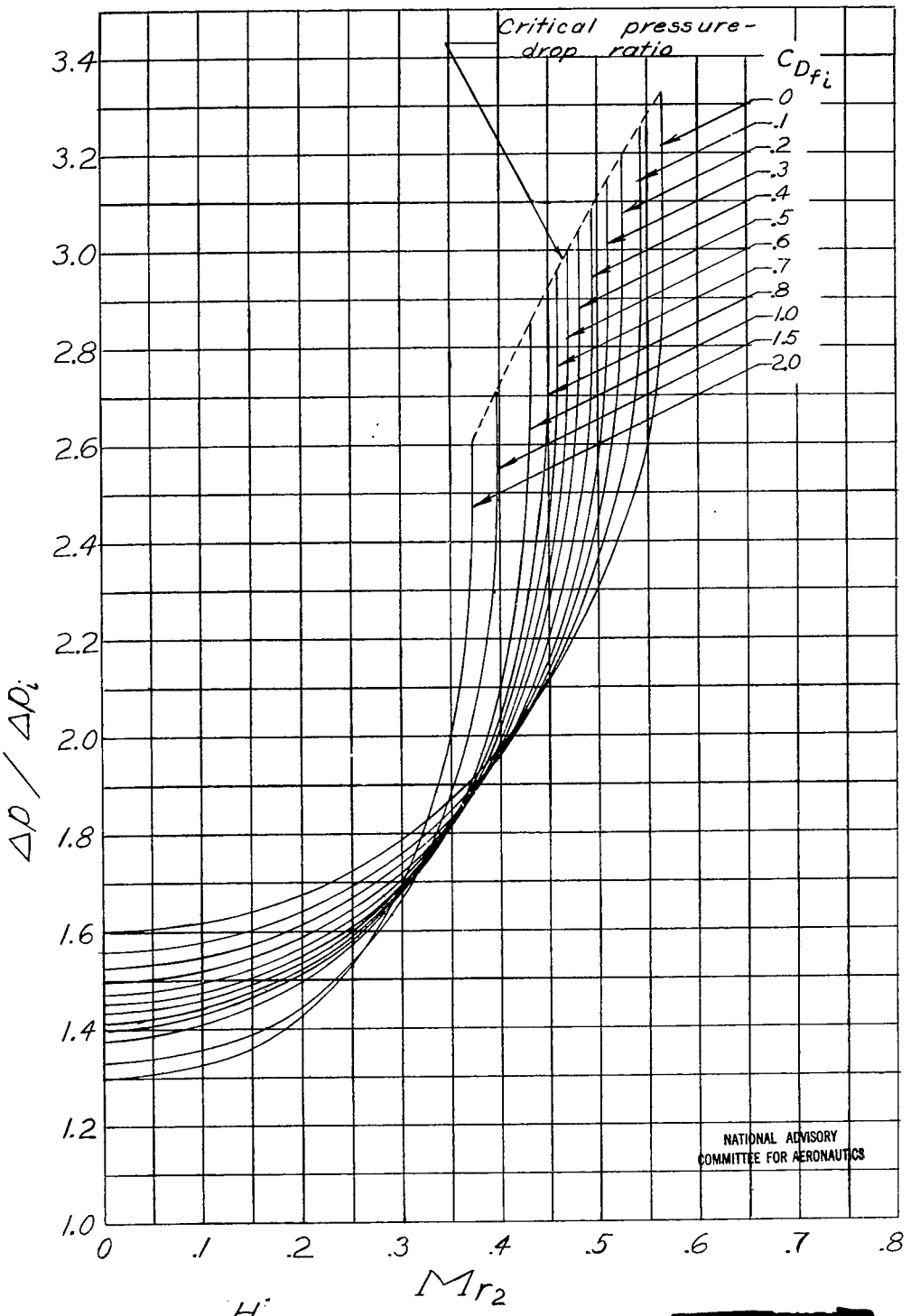

(f) $\frac{H'}{c_p g m T_{r_2}} = 0.30.$ [redacted]

Figure 5.- Continued.

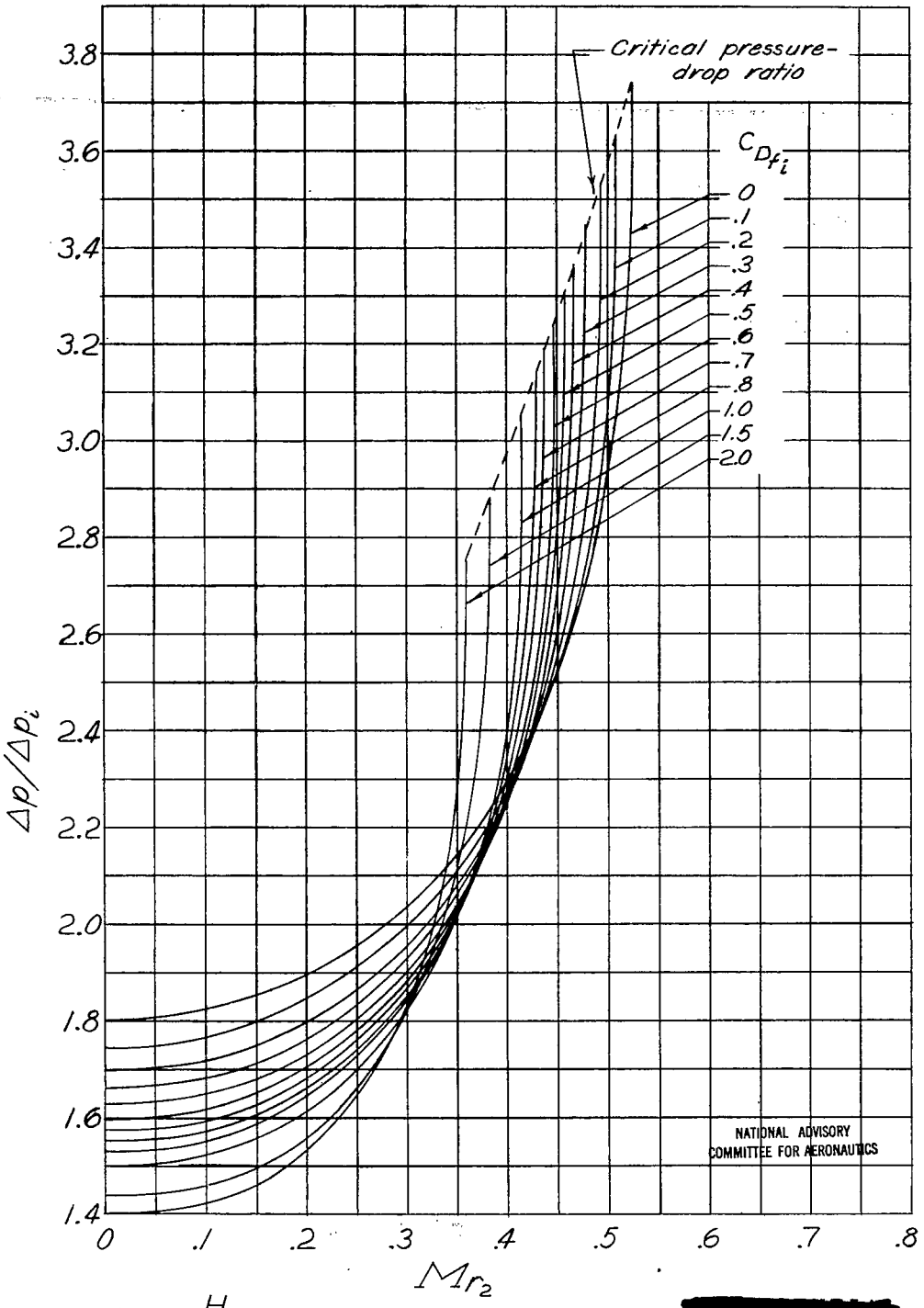

(g) $\frac{H}{c_p g m T_{r_2}} = 0.40.$

Figure 5 .- Concluded.

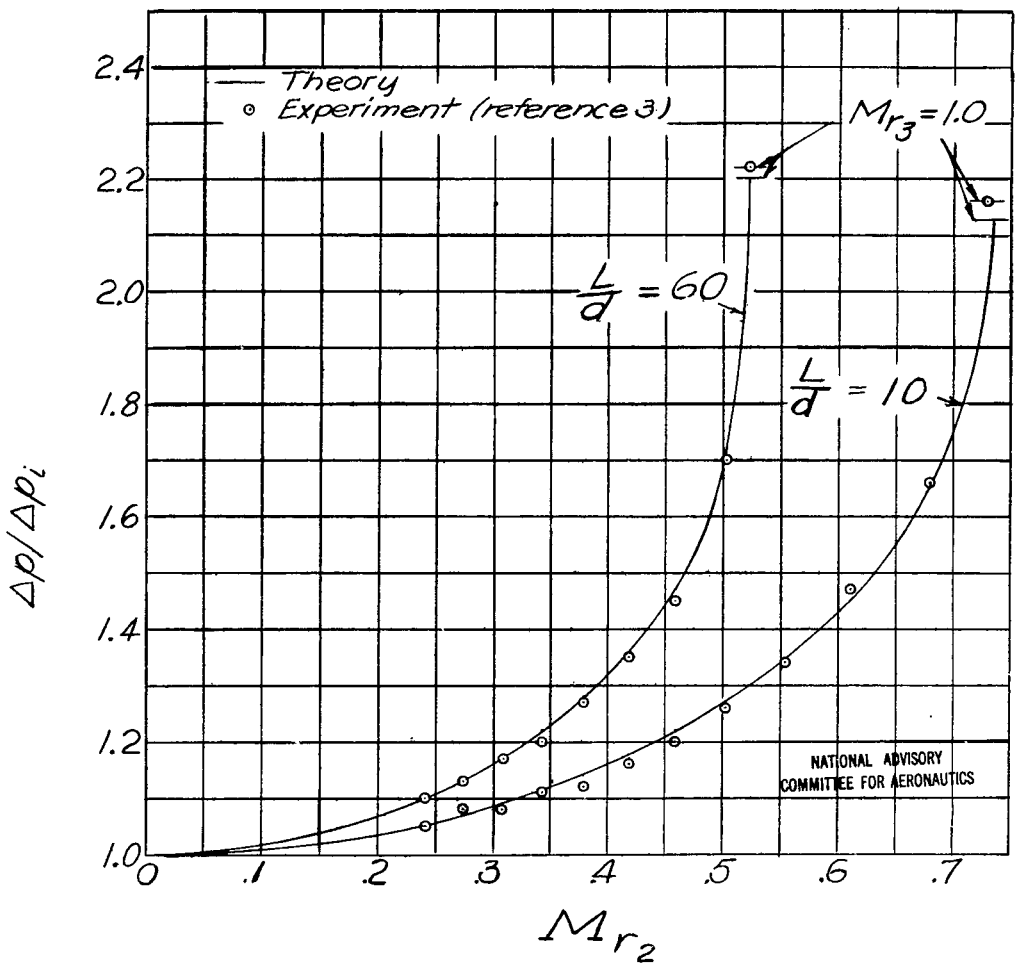

Figure 6.- Comparison of theoretical variation of pressure-drop ratio with experimental data obtained from reference 3.

[redacted]

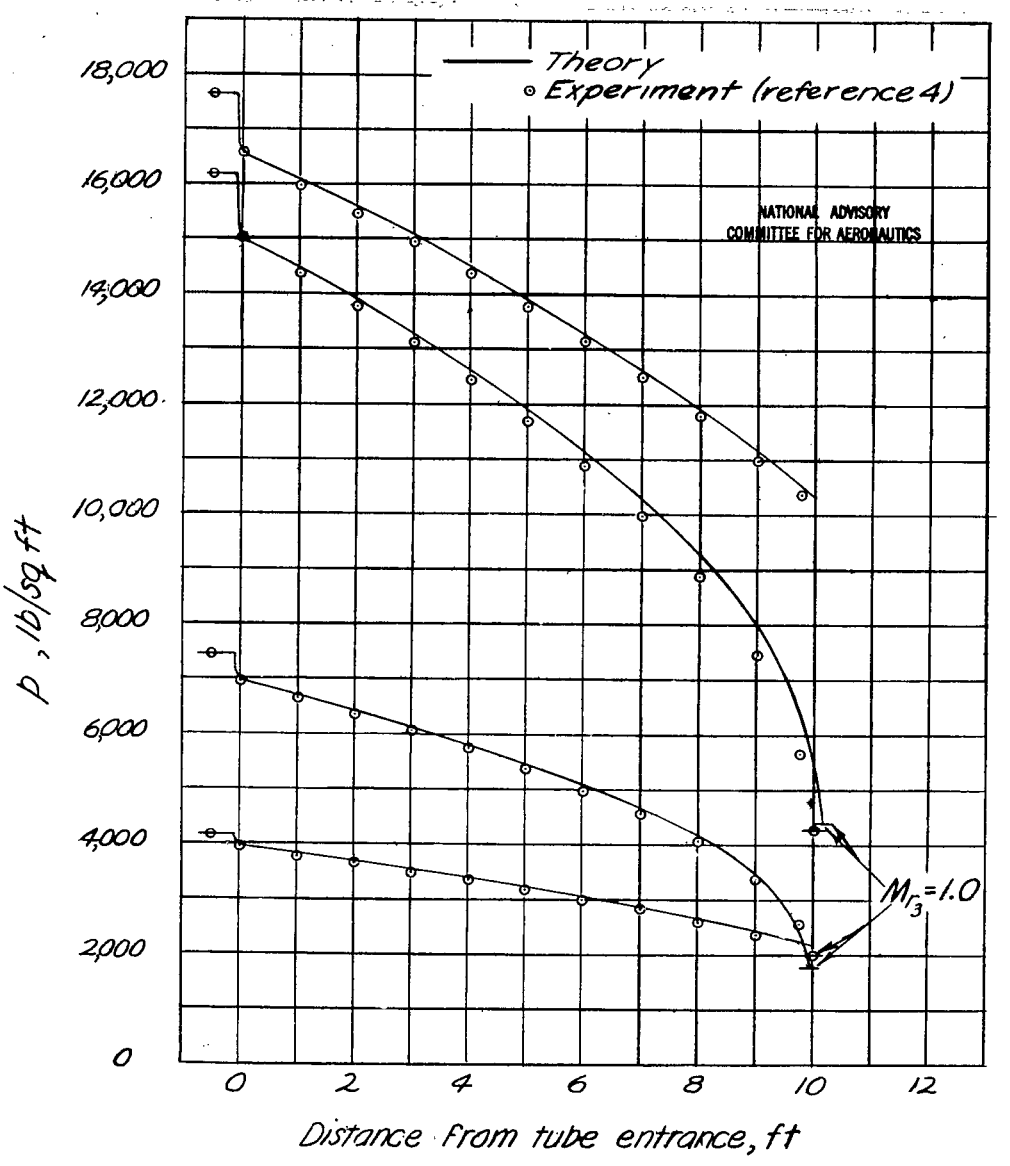

Figure 7.-Comparison of theoretical and experimental pressure drop along the 3/8-inch by 10-foot tube of reference 4.

[redacted]

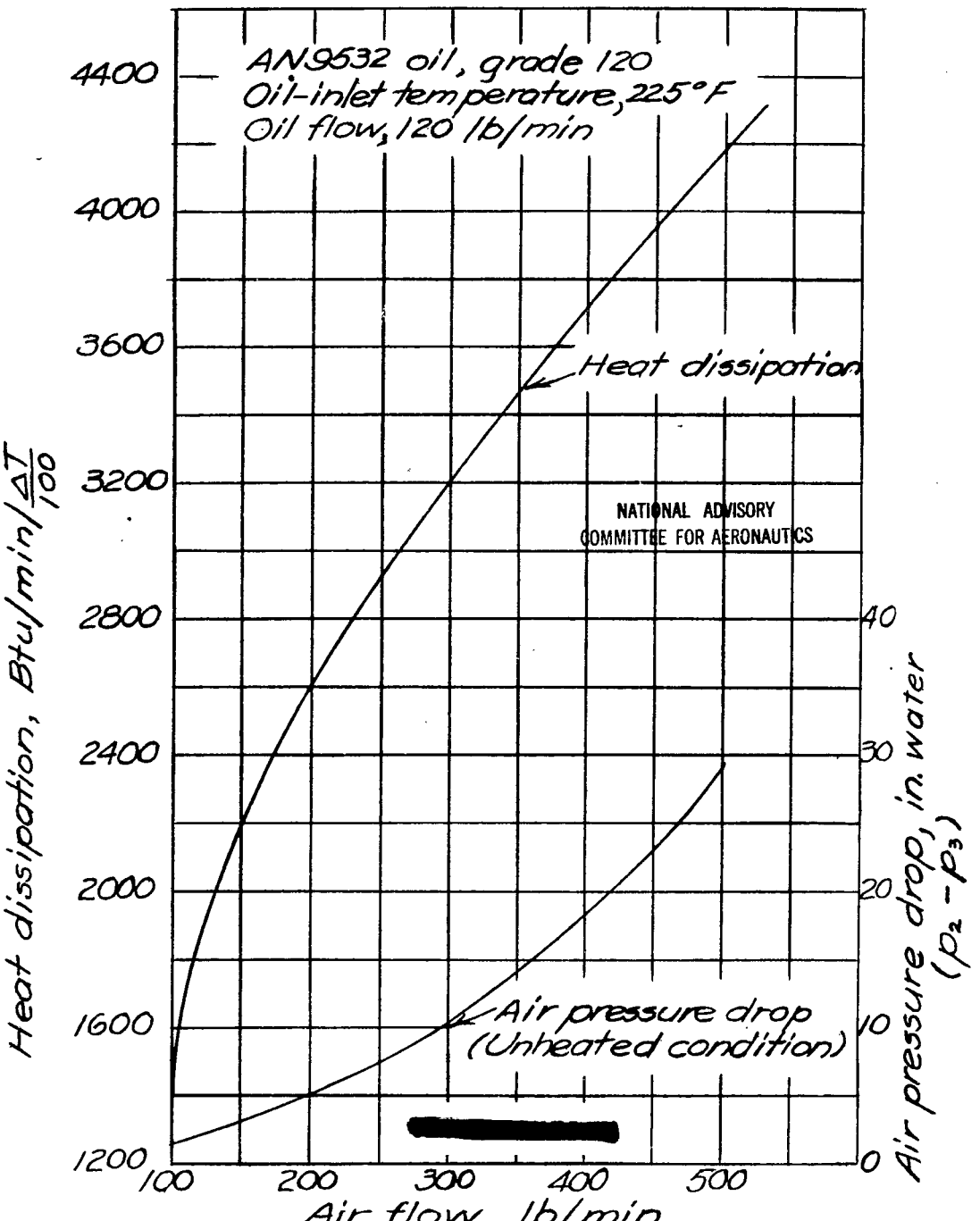

Figure 8.—Oil-cooler data used in illustrative example. 12-inch-diameter cooler with 0.210-by 12-inch tubes. Air-inlet temperature, 100°F; density, 0.0765 pounds per cubic foot. (ΔT = Average oil temperature minus inlet-air temperature)